Membrane and Water Treatment, *Vol. 17, No. 4 (2026) 333-342*
https://doi.org/10.12989/mwt.2026.17.4.333

Techno-Press

Gated flow in nanopores for liquid-liquid separation

Yongbin Zhang*

College of Mechanical Engineering, Changzhou University, Changzhou, 213164, Jiangsu Province, China

(Received April 20, 2026, Revised July 6, 2026, Accepted July 7, 2026)

Abstract. The nanopores with small radii (R) and long axial lengths (l) were found to be on or off for the fluid flow, dependent on the external power loss. The value of R may be no more than 1nm, and the ratio l/R can be on the scales 1.0E+3 or 1.0E+4. In the case of a small power loss, no wall slippage occurs and the flow resistance of the nanopore is huge so that the flow rate through the nanopore is as small as negligible. When the power loss on the nanopore is high enough, the wall slippage occurs and the flow resistance of the nanopore approaches to vanishing so that the flow rate through the nanopore is large. These functions are important for the liquid-liquid separation by using nanoporous filtration membranes. For the two mixed liquids, if the critical power losses on the nanopore for wall slippage is greatly different, one liquid can smoothly flow through the nanopore while the other liquid is impeded from flowing through it when the magnitude of the power loss exerted on the nanopore is between the two critical power losses for wall slippage.

Keywords: flow resistance; hydrophobic; nanopore; power loss; separation; wall slippage

1. Introduction

The liquid-liquid separation is challenging in the membrane filtration. It normally relies on the great difference in the physical properties (density, immiscibility or/and boiling point) of two liquids. The normal method for the liquid-liquid separation is the gravity separation [1], the centrifugal separation [2], the extraction [3] and the distillation [4] etc.

Nanoporous filtration membranes have been developed fast for realizing fine filtration or ultra filtration [5-7]. The radii of the nanopores of these membranes can be on the scales of 1-100nm. These membranes are normally used to separate the very small impurities from the liquid, like used in the water purification [8, 9] and the hemofiltration [10]. Their functions are dependent on the size of the nanopore. Over small nanopores such as with the radius on the 1nm scale can realize the ultra refinement but normally have much smaller fluxes because of the over large flow resistances.

However, peculiar phenomena were observed inside the very small nanopores. Experiments and molecular dynamics simulations showed that the water flow rates through the carbon nanopores with the diameters below 7nm were several orders higher than the classical hydrodynamic flow theory calculation [11-15]. Moreover, smaller the nanopore diameter, more pronounced the flow enhancement [16]. These phenomena are unexplainable from the classical fluid mechanics, which calculates the large flow resistance of the small nanochannels and far lower flow rates. They

*Corresponding author, Professor, E-mail: engmech1@sina.com

ISSN: 2005-8624 (Print), 2092-7037 (Online)

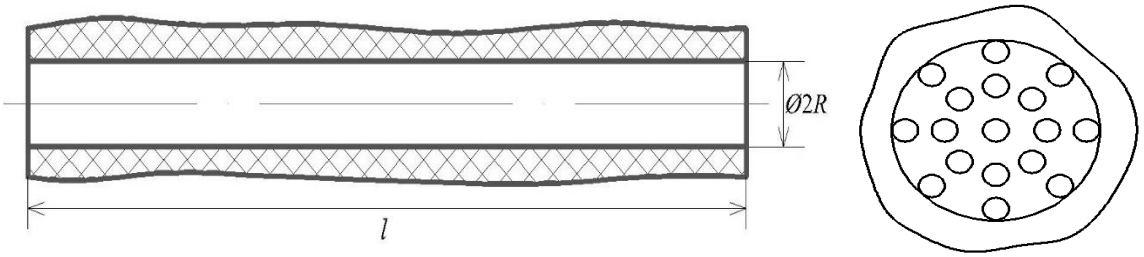

(a) Local section view (b) Local front view

Figure 1. The nanopore with a large value of l/R

have been ascribed to the great wall slippage resulting from the hydrophobic nanopore wall. Wang and Zhang [17] suggest that there are three mechanisms governing the fluid flow through the very small nanopore i.e. the wall slippage, the fluid non-continuum property and the fluid viscosity enhancement. The combined effects of these three factors are determined by the power loss (*POW*) on the whole nanopore. A suffciently high value of *POW* makes the wall slippage effect dominant and thus results in the unexpectedly high flow rate through the nanopore. While a small value of *POW* can not generate the wall slippage and the other two factors severely impede the fluid flow through the nanopore.

The present paper proposes the specific nanoporous filtration membrane which can be used for the liquid-liquid separation. The radius of the nanopore of this membrane is on the 1nm scale and the ratio of the axial length to the radius of the nanopore is on the scales of 1.0E+3 or 1.0E+4. The critical power losses on the nanopore for starting the wall slippage for the two liquids are quite different. When the exerted power loss on the nanopore ranges between these critical power losses of the two liquids, one liquid can not flow through the nanopore because of the absence of the wall slippage and the huge flow resistance, while the other liquid can fluently flow through the nanopore because of the occurrence of the wall slippage and the far lower flow resistance. Thus, the two liquids can be separated from one another by using this membrane.

2. Nanopores with large values of l/R

Fig. 1 shows the studied long nanopore with the large ratio (l/R) of the axial length to the radius, which may be over 1000. For the water flow, the value of the nanopore radius R may be no more than 1nm, however the axial length l of the nanopore may be more than 1μm. The filtration membrane with such geometrical configurations of the nanopore not only possesses the ultra filtration but also has the much improved mechanical strength. The classical Hagen-Poiseuille equation gives that the flow resistance of this nanopore is very large and the flow rate through the nanopore is normally as small as negligible. However, the experiment [14] showed that the water flow rate through the carbon nanopore with the geometrical configuration shown by Fig. 1 was actually 2 to 3 orders higher than the classical flow theory calculation. The ultra fast water flow was ascribed to the wall slippage [12-14, 16]. It appears that the flow resistances of the nanopore in Fig. 1 are largely different when the wall slippage occurs or not.

3. Flow resistance of and mass flow rate through the nanopore

3.1 For no wall slippage

The flow resistance of the nanopore is defined as:

$$i_f = \frac{|\Delta p|}{q_m} \tag{1}$$

Define the dimensionless flow resistance of the nanopore as $I_f = i_f / i_{f0}$, where $i_{f0} = 4\eta/(\pi\rho R_0^3)$. If no wall slippage occurs, the mass flow rate through the nanopore in Fig. 1 is [18]:

$$q_m = \frac{\pi\rho_{bf}^{eff} SR^4}{4\eta_{bf}^{eff}} \frac{\partial p}{\partial x} \tag{2}$$

If no wall slippage occurs, the dimensionless flow resistance of the nanopore in Fig. 1 is thus finally expressed as:

$$I_{f,\max} = -\frac{LC_y}{SC_q \lambda_R^3} \tag{3}$$

If no wall slippage occurs, the mass flow rate through the nanopore in Fig. 1 is:

$$q_m = \sqrt{\frac{\rho C_q POW}{I_{f,\max} i_{f0}}} \tag{4}$$

3.2 For the case of wall slippage

If the wall slippage occurs, the mass flow rate through the nanopore in Fig.1 is [18]:

$$q_m = \pi\rho_{bf}^{eff} u_s R^2 + \frac{\pi\rho_{bf}^{eff} SR^4}{4\eta_{bf}^{eff}} \frac{\partial p}{\partial x} \tag{5}$$

where the wall slipping velocity is expressed as [19]:

$$u_s = \frac{(POW - POW_{cr})\theta_\tau}{\pi\tau_s lR} \tag{6}$$

By substituting Eq. (6) into Eq. (5), if the wall slippage occurs, the dimensionless flow resistance of the nanopore in Fig. 1 is finally expressed as:

$$I_f = \frac{I_{f,\max}}{x_{pow}}, \quad \text{for } x_{pow} \geq 1 \tag{7}$$

where $x_{pow} = POW/POW_{cr}$

If the wall slippage occurs, the mass flow rate through the nanopore in Fig. 1 is:

$$q_m = POW\sqrt{\frac{\rho C_q}{I_{f,\max} i_{f0} POW_{cr}}}, \quad \text{for } x_{pow} \geq 1 \tag{8}$$

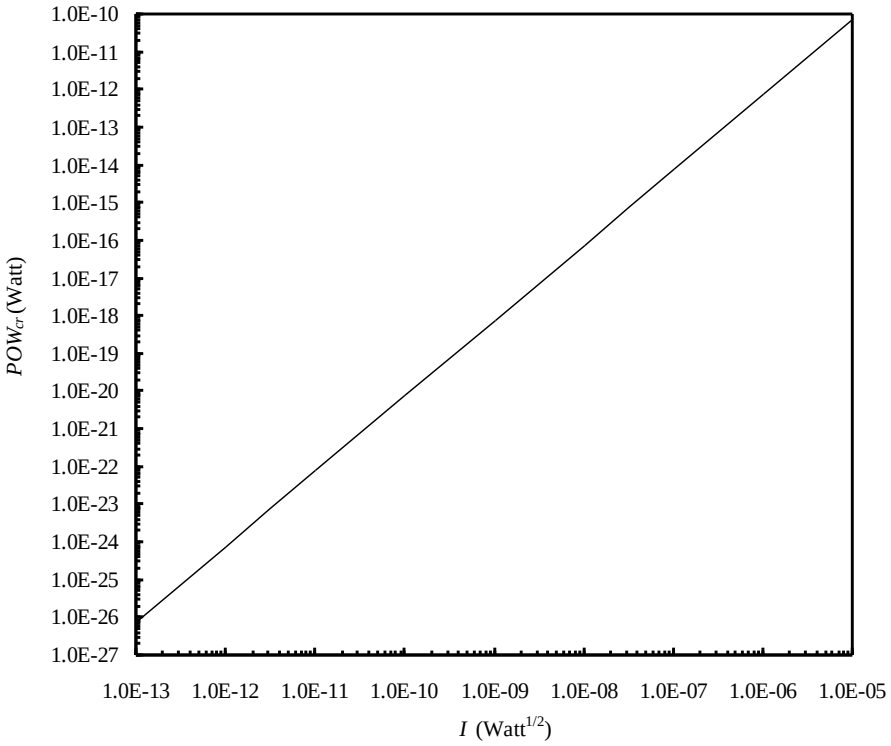

Figure 2. Values of POW_{cr} as function of the intrinsic parameter I for a weak fluid-pore wall interaction

3.3 General expressions for the dimensionless flow resistance of and the mass flow rate through the nanopore

According to Eqs. (3, 7), the dimensionless flow resistance of the nanopore in Fig. 1 is generally expressed as:

$$\frac{I_f}{I_{f,\max}} = \begin{cases} 1, \text{ for } x_{pow} \le 1 \\ \dfrac{1}{x_{pow}}, \text{ for } x_{pow} \ge 1 \end{cases} \tag{9}$$

According to Eqs. (4, 8), the mass flow rate through the nanopore in Fig. 1 is generally expressed as:

$$\frac{q_m}{q_{m,cr}} = \begin{cases} \sqrt{x_{pow}}, \text{for } x_{pow} \le 1 \\ x_{pow}, \text{for } x_{pow} \ge 1 \end{cases} \tag{10}$$

where

$$q_{m,cr} = I\sqrt{-\frac{\pi S\rho C_q}{4C_y\theta_\tau^2 I_{f,\max}\dot{I}_{f0}}} \tag{11}$$

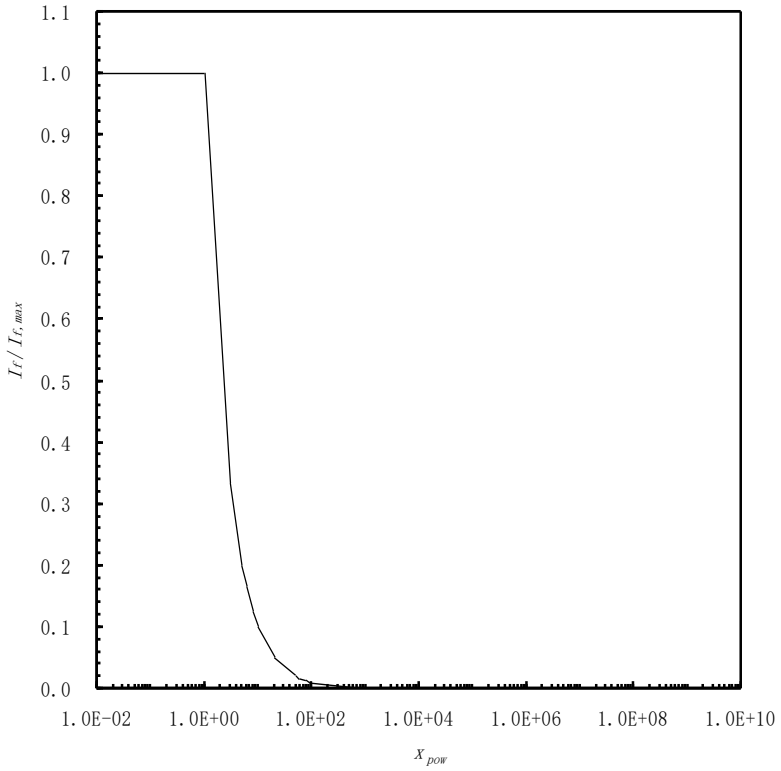

Figure 3. Values of $I_f/I_{f,max}$

4. Results

For achieving a specific performance of the flow resistance of the long nanopore shown in Fig. 1 with varying power loss POW, the fluid-pore wall interaction must be weak so that the value of POW_{cr} is low. For example, the nanopores made of carbon or graphene are hydrophobic, and the water-tube wall interaction is weak. For these cases, $C_q \approx 1$, $C_y \approx 1$, $\theta_\tau \approx 1$, and $S \approx -1$. Fig. 2 shows the calculated values of POW_{cr} for a weak fluid-pore wall interaction. For the water flow in a carbon nanopore, τ_s on the scale of 10 kPa, $\eta = 0.001\text{Pa} \cdot s$, and the values of I are on the scales from 1.0E-7 Watt$^{1/2}$ to 1.0E-5 Watt$^{1/2}$ when $R = 1\text{nm}$ and $l = 1\mu\text{m} - 1000\mu\text{m}$. It can be seen from Fig. 2 that the corresponding values of POW_{cr} are on the scales from 1.0E-15 Watt to 1.0E-11Watt.

Fig. 3 shows the values of $I_f/I_{f,max}$ as function of x_{pow}. For $x_{pow} \leq 1$, no wall slippage occurs and the dimensionless flow resistance I_f of the nanopore is equal to $I_{f,max}$, which is very large and on the scales from 1.0E+6 to 1.0E+9 when $l = 1\mu\text{m} - 1000\mu\text{m}$, $R = 1\text{nm}$ and R_0=10nm.

$1 \leq x_{pow} \leq 100$ is the transition zone where the value of $I_f/I_{f,max}$ is very rapidly reduced with the increase of x_{pow}. $x_{pow} \geq 100$ is the zone where the values of $I_f/I_{f,max}$ approach to vanishing. Fig. 3 shows the two important working zones of the nanopore where the flow resistances of the nanopore are respectively very large and very low. In which zone the nanopore

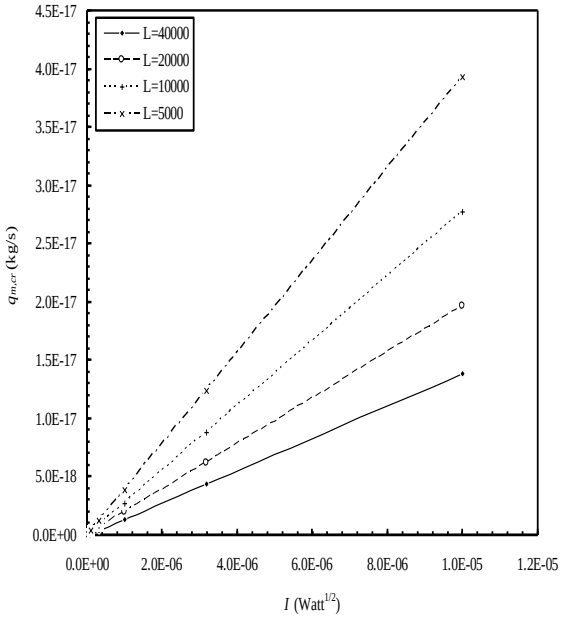

(a) R = 0.5nm

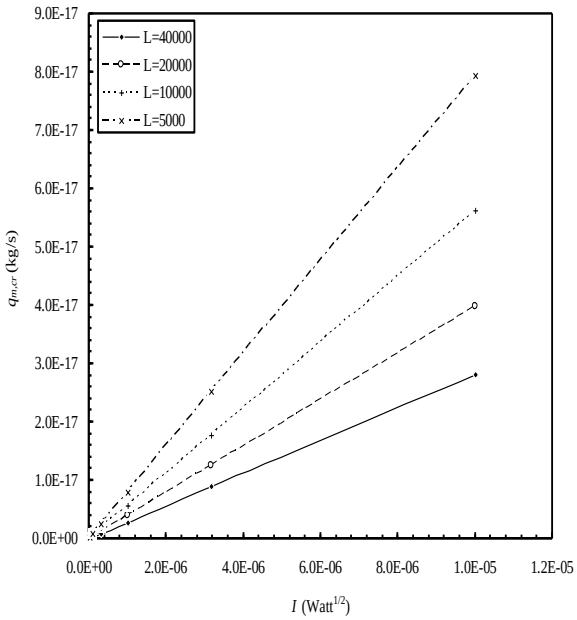

(b) R = 0.8nm

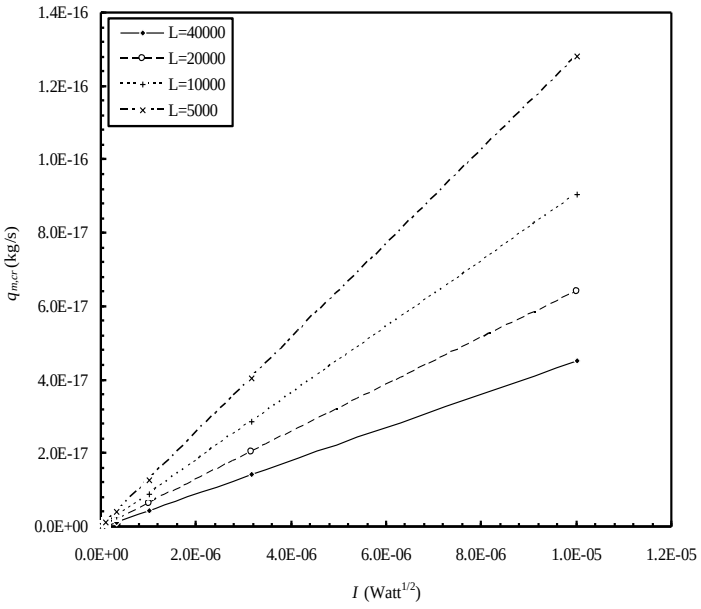

(c) $R = 1.1nm$

Figure 4. Values of $q_{m,cr}$ for a weak fluid-pore wall interaction

works entirely depends on the value of x_{pow} i.e., the power loss exerted on the whole nanopore. This flow resistance performance of the nanopore indicates the gated transport in the nanopore controlled by the applied power. It is a very important function for the liquid-liquid separation. Figs. 4(a-c) show the dimensional values of the mass flow rate $q_{m,cr}$ through the nanopore for

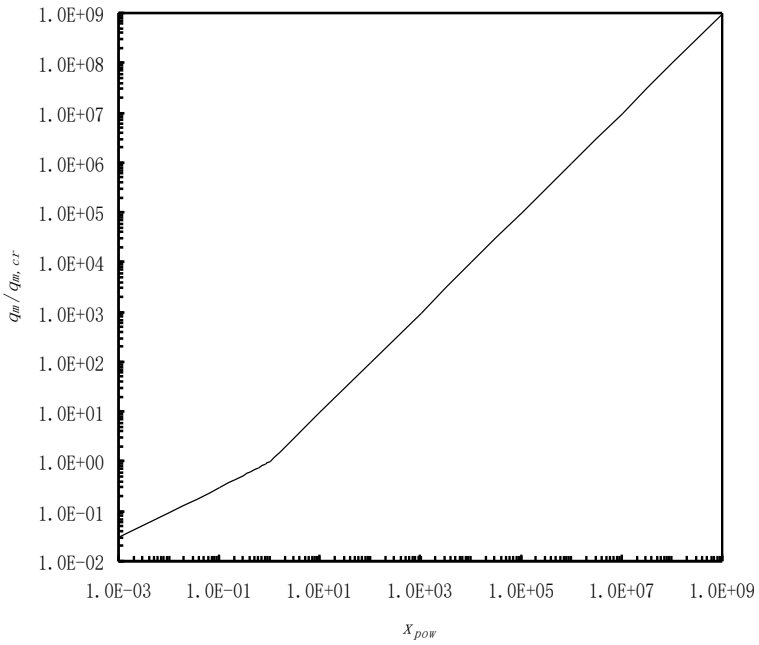

Figure 5. Values of $q_m/q_{m,cr}$

different *I*, *L* and *R* when the power loss on the nanopore is equal to the critical value for initiating the wall slippage i.e. $POW = POW_{cr}$. The value of $q_{m,cr}$ is the highest mass flow rate through the nanopore when the nanopore has the largest dimensionless flow resistance $I_{f,max}$ in working. For *R*=0.5nm-1.1nm and *L*=5000-40000, the values of $q_{m,cr}$ are no more than 1.4E-16kg/s when *I*=1.0E-7 Watt$^{1/2}$ to 1.0E-5 Watt$^{1/2}$. For the total number of the nanopores *N*=1.0E+11, the total values of $q_{m,cr}$ through these nanopores are no more than 0.014 g/s, which is so small to be negligible as occurring in a nanoporous filtration membrane. Thus, when no wall slippage occurs, the flow resistance of the nanopore is very large so that the liquid like water can not flow through the nanopore.

Fig. 5 shows that when $x_{pow} \leq 1$ i.e., no wall slippage occurs, $q_m/q_{m,cr} \leq 1$; However, when $x_{pow} > 1$ i.e., the wall slippage occurs, the value of $q_m/q_{m,cr}$ is on the same scale with x_{pow}. It means that if POW_{cr} is very low, even for a very modest value of POW, the value of x_{pow} is on several orders and thus q_m is several orders higher than $q_{m,cr}$. This indicates that the nanopore can be opened so that the liquid can fast flow through it just by applying sufficiently high power loss on the nanopore. These suggest that the nanopore is on or off in transport by the exerted power loss on it.

5. Indication of the function of the nanoporous filtration membrane for the liquid-liquid separation

The above results indicate that if the values of the radius *R* and the ratio *l*/*R* of the nanopore in a nanoporous filtration membrane hold the above mentioned characteristics, the inside wall of the

nanopore is so designed that the critical power losses on the nanopore for starting the wall slippage respectively for the two liquids are quite different, and in operation the power loss exerted on the nanopore ranges between these two critical power losses, one liquid will not flow through the nanopore because of the exerted power loss smaller than its critical power loss for the wall slippage, while the other liquid will flow through the nanopore smoothly because of the exerted power loss greater than its critical power loss for the wall slippage. The two liquids can thus be separated from one another. It forms the principle of the liquid-liquid separation of the present addressed specific nanoporous filtration membrane.

6. Conclusions

The paper proposes the long hydrophobic nanopore with the small radius no more than 1nm as the gated nanopore. The ratio of the axial length of this nanopore to its radius can be on the scales 1.0E+3~1.0E+4 or even more. In the absence of the wall slippage, the flow resistance of this nanopore is very large and the liquid can not flow through it, as described by the classical hydrodynamic flow theory. However, if the nanopore wall is highly hydrophobic so that the fluid-nanopore wall interfacial shear strength is low, the critical power loss on the whole nanopore for initiating the wall slippage is low, and only a modest power loss on the whole nanopore can open the nanopore with a high flux by generating the great wall slippage. Whether this nanopore is closed or opened is entirely determined by the exerted power loss on the nanopore, which also determines the flux through the opened nanopore. These functions are indeed critically important for realizing the liquid-liquid separation by using the nanoporous filtration membrane. That is: if we exert the power loss on the nanopore which ranges between the critical power losses on the nanopore for starting the wall slippage respectively for the two liquids, the liquid with the higher critical power loss for the wall slippage can not flow through the nanopore because of the absence of the wall slippage, while the other liquid with the smaller critical power loss for the wall slippage can smoothly flow through the nanopore because of the wall slippage occurrence. This forms the principle of the liquid-liquid separation of the present addressed specific nanoporous filtration membrane.

References

1. Farajzadeh, S., Chehreh, C.S. (2022). Gravity separation by falcon concentrator- an over review. Separation Science Technology, 57, 2145-2164. https://doi.org/10.1080/01496395.2022.2028836.
2. Brouwers, J.J.H. (2023). Innovative methods of centrifugal separation. Separation, 10, 181. https://doi.org/10.3390/separations10030181.
3. Bokhary, A., Leitch, M., Liao, B.Q. (2021). Liquid-liquid extraction technology for resource recovery: Applications, potential, and perspectives. Journal of Water Process Engineering, 40, 101762. https://doi.org/10.1016/j.jwpe.2020.101762.
4. Curcio, E., Drioli, E. (2005). Membrane distillation and related operations—A review. Separation and Purification Review, 34, 35-86. https://doi.org/10.1081/SPM-200054951.
5. Ariono, D., Aryanti, P.T.P., Wardani, A.K., Wenten, I.G. (2018). Fouling characteristics of humic substances on tight polysulfone-based ultrafiltration membrane. Membrane and Water Treatment, 9, 353-361. https://doi.org/10.12989/mwt.2018.9.5.353.
6. El-ghzizel, S., Jalté, H., Zeggar, H., Zait, M., Belhamidi, S., Tiyal, F., Hafsi, M., Taky, M., Elmidaoui,

A. (2019). Autopsy of nanofiltration membrane of a decentralized demineralization plant. Membrane and Water Treatment, 10, 277-286. https://doi.org/0.12989/mwt.2019.10.4.277.
7. Surwade, S.P., Smirnov, S.N., Vlassiouk, I.V., Unocic, R.R., Veith, G.M., Dai, S., Mahurin, S.M. (2015). Water desalination using nanoporous single-layer grapheme. Nature Nanotechnology, 10, 459-464. https://doi.org/10.1038/nnano.2015.37.
8. Bottino, A., Capannelli, G., Comite, A., Ferrari, F., Firpo, R. (2011). Water purification from pesticides by spiral wound nanofiltration membrane. Membrane and Water Treatment, 2, 63-74. http://doi.org/10.12989/mwt.2011.2.1.063.
9. Cohen-Tanugi, D., Lin, L.C., Grossman, J.C. (2016). Multilayer nanoporous graphene membranes for water desalination. Nano Letter, 16, 1027. https://doi.org/10.1021/acs.nanolett.5b04089.
10. Fissel, W.H., Dubnisheva, A., Eldridge, A.N., Fleischman, A.J., Zydney, A.L., Roy, S. (2009). High-performance silicon nanopore hemofiltration membranes. Journal of Membrane Science, 326, 58-63. http://doi.org/10.1016/j.memsci.2008.09.039.
11. Borg, M.K., Reese, J.M. (2017). Multiscale simulation of enhanced water flow in nanotubes. MRS Bulletin, 42, 294-299. https://doi.org/10.1557/mrs.2017.59.
12. Holt, J.K., Park, H.G., Wang, Y., Stadermann, M., Artyukhin, A.B., Grigoropoulos, C.P., Noy, A., Bakajin, O. (2006). Fast mass transport through sub-2-nanometer carbon nanopores. Science, 312, 1034-1037. https://doi.org/10.1126/science.1126298.
13. Majumder, M., Chopra, N., Andrews, R., Hinds, B.J. (2005). Enhanced flow in carbon nanopores. Nature, 438, 44. https://doi.org/10.1038/438044a.
14. Qin, X.C., Yuan, Q., Zhao, Y., Xie, S., Liu, Z. (2011). Measurement of the rate of water translocation through carbon nanopores. Nano Letter, 11, 2173-2177. https://doi.org/10.1021/nl200843g.
15. Wang, L.Y., Dumont, R.S., Dickson, J.M. (2012). Nonequilibrium molecular dynamics simulation of water transport through carbon nanotube membranes at low pressure. Journal of Chemical Physics, 137, 044102. https://doi.org/10.1063/1.4734484.
16. Secchi, E., Marbach, S., Niguès, A., Stein, D., Siria, A., Bocquet, L. (2016). Massive radius-dependent flow slippage in carbon nanopores. Nature, 537, 210-213. https://doi.org/10.1038/nature19315.
17. Wang, M., Zhang, Y.B. (2025). Mass flow in nanoporous filtration membrane with small nanopores. Membrane and Water Treatment, 16, 187-194. https://doi.org/10.12989/mwt.2025.16.4.187.18.
18. Zhang, Y.B. (2017). Transport in nanopore tree. International Journal of Heat and Mass Transfer, 114, 536-540. https://doi.org/10.1016/j.ijheatmasstransfer.2017.06.105.
19. Wang, M., Zhang, Y.B. (2021). Water transport in cellular connexon of human bodies. Frontier in Heat and Mass Transfer, 17, 9. https://doi.org/10.5098/hmt.17.9.

Nomenclature

$C_q = \dfrac{\rho_{bf}^{eff}}{\rho}$

$C_y = \dfrac{\eta_{bf}^{eff}}{\eta}$

$I = \tau_s R\sqrt{l/\eta}$

$L = l/R$

p pressure, Pa

POW power loss on the whole nanopore, Watt

POW_{cr} critical power loss on the whole nanopore for initiating the wall slippage, $-\pi SI^2/(4C_y\theta_\tau^2)$ [19],

Watt

q_m mass flow rate through the nanopore, kg/s

$q_{m,cr}$ mass flow rate through the nanopore when $POW = POW_{cr}$, kg/s

R_0 reference radius, m

S parameter accounting for the non-continuum effect across the pore radius $(-1 \leq S < 0)$

u_s wall slipping velocity, m/s

x coordinate in the pore axial direction, m

$x_{pow} = POW/POW_{cr}$

$\lambda_R = R/R_0$

η fluid bulk dynamic viscosity, Pa s

ρ fluid bulk density, kg/m^3

$\rho_{bf}^{eff}, \eta_{bf}^{eff}$ average density and effective viscosity across the pore radius respectively, kg/m^3, Pa s

θ_τ correction factor for the wall shear stress due to the non-continuum effect across the pore radius

τ_s fluid-pore wall interfacial shear strength, Pa

Δp pressure drop on the whole nanopore, Pa